Available online at www.sciencedirect.com
ScienceDirect
Mendeleev Commun., 2016, **26**, 335–337
Mendeleev Communications

Synthesis and optical and photocatalytic properties of manganese-doped titanium oxide with a three-dimensional architecture of particles

Inna V. Baklanova,* Vladimir N. Krasil'nikov, Olga I. Gyrdasova and Larisa Yu. Buldakova

Institute of Solid State Chemistry, Ural Branch of the Russian Academy of Sciences, 620990 Ekaterinburg, Russian Federation. E-mail: baklanova_i@ihim.uran.ru

DOI: 10.1016/j.mencom.2016.07.023

The solid solutions $Ti_{1-x}Mn_xO_{2-x}$ ($0.003 \leqslant x \leqslant 0.016$) with a 3D architecture of particles exhibiting high photocatalytic activity under both ultraviolet and visible irradiation have been synthesized using $Ti_{1-x}Mn_x(OCH_2CH_2O)_{2-x}$ as a precursor.

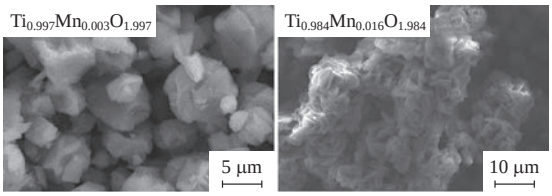

Photocatalysts based on nanosized titanium dioxide are of interest because of the prospects of their use for the removal of organic contaminants, fungi and malignant bacteria from wastewater. A disadvantage of such materials is the band gap of TiO_2 (3.0 eV for rutile or 3.2 eV for anatase), which restricts its application only to the UV range. Among the most widespread structural modifications of titanium dioxide, anatase demonstrates the highest photocatalytic activity, which is due to a strong tendency of its particles to hydroxylation. The optical response of anatase can be expanded into the visible region due to its doping with metals or nonmetals.[1] Doping with transition metal ions leads to the formation of new energy levels in the band gap of TiO_2 acting as electron traps. Electron capture can decrease the rate of recombination of the exciton pair ($h^+ + e^-$) during irradiation and thereby increase the lifetime of charge carriers. Moreover, doping with metals enhances light absorption in the visible region owing to band gap narrowing. Earlier, it was noted that an inconsiderable concentration of manganese in titanium dioxide increased the photocatalytic activity of a photocatalyst in the UV and visible spectral regions.[1–4] The prospects of manganese as a dopant probably result from the fact that it has several valence states, which may trap electrons or holes giving rise, for example, to superoxide (O_2^-) and hydroxide ($^{\bullet}OH$) radicals promoting the catalyst photoactivity. However, the nature of a manganese effect on the photocatalytic activity of titanium dioxide is debatable since there are explicitly contrary opinions.[5] At the same time, the disagreement is caused by a variety of methods of the synthesis of manganese-doped samples, which affects the morphology, size and specific surface area of particles and leads to a variety of physical and functional properties of produced items. Therefore, it is very important to choose an appropriate synthesis method and an optimal concentration of manganese for increasing the photocatalytic effect under UV and visible irradiation. The precursor method, as distinct from other synthetic techniques, has many advantages, namely, simplicity, quick reaction capability, low operating temperatures, and control over the particle shape and size.[6] It allows one to achieve the uniform dispersion of doping metal ions in a structural matrix of titanium dioxide and to control the stoichiometry of produced materials. Thus, using the $Ti_{1-x}Me_x(OCH_2CH_2O)_2$ glycolate as a precursor, we synthesized titanium dioxide doped with metals and simultaneously with metals and carbon in the form of nanodispersed solid solutions with the controllable dimensions and morphological characteristics of particles.[7–12] Hence, in order to elucidate the effect of manganese doping and its concentration on the photoactivity of titanium dioxide, it is necessary to employ a comprehensive approach combining the choice of synthesis method and control over all stages with thorough examination of the physicochemical properties of synthesized products.

For the synthesis of the samples, $Ti_{1-x}Mn_x$-$(OCH_2CH_2O)_{2-x}$ ($0.003 \leqslant x \leqslant 0.016$) was used as a precursor taking into consideration the ability of its crystal aggregates to undergo a pseudomorphic transformation into $Ti_{1-x}Mn_xO_{2-x}$ oxide particles on heating in air. The precursors were prepared by crystallization from a hot solution of titanium tetrabutoxide $Ti(OBu)_4$ and manganese formate $Mn(HCOO)_2 \cdot 2H_2O$ in ethylene glycol, for which the following reactions are typical:

$$Ti(OBu)_4 + 2(CH_2OH)_2 = Ti(OCH_2CH_2O)_2 + 4BuOH, \quad (1)$$

$$Mn(HCOO)_2 \cdot 2H_2O + (CH_2OH)_2 = Mn(OCH_2CH_2O) + 2HCOOH + 2H_2O. \quad (2)$$

When reactions (1) and (2) occur simultaneously, glycolate $Ti_{1-x}Mn_x(OCH_2CH_2O)_{2-x}$ is formed due to the partial replacement of manganese with titanium in the structure of $Ti(OCH_2CH_2O)_2$. The samples of $Ti_{1-x}Mn_x(OCH_2CH_2O)_{2-x}$ ($0.003 \leqslant x \leqslant 0.016$) have been synthesized. As distinct from white $Ti(OCH_2CH_2O)_2$, they have a pink color, which becomes more intense as the concentration of manganese grows. It is important that reaction (2) proceeds *via* the formation of the $Mn(HCOO)_2(HOCH_2CH_2OH)$ solvate as an intermediate, whose needle crystals precipitate from the solution of manganese formate in ethylene glycol after exposure at a temperature of about 100 °C. In order to produce manganese-doped titanium dioxide in the form of $Ti_{1-x}Mn_xO_{2-x}$ solid solutions free of carbon impurities, the precursors were annealed in air at 500 °C for 4 h.

According to the X-ray phase analysis and oscillation spectroscopy data,† the synthesized $Ti_{1-x}Mn_x(OCH_2CH_2O)_{2-x}$ precursors ($0.003 \leqslant x \leqslant 0.016$) were individual phases isostructural to titanium glycolate $Ti(OCH_2CH_2O)_2$.[10,13] The vibrational spectra of $Ti(OCH_2CH_2O)_2$ and $Ti_{1-x}Mn_x(OCH_2CH_2O)_{2-x}$ synthesized by the above method differed from each other only in a slight shift induced by the effect of the dopant cation. The lines at

2930, 2909 and 2858 cm^{-1} in the Raman spectrum of mixed glycolate with $x = 0.016$ are due to the asymmetrical and symmetrical stretching vibrations of the C–H bonds in the CH_2 groups observed in the Raman spectrum of ethylene glycol.[14,15] The lines at 1467 cm^{-1} and at 1359 and 1343 cm^{-1} are ascribed to the asymmetrical and symmetrical bending vibrations of C–H bonds, respectively. The lines at 1219 and 1236 cm^{-1} correspond to the radial bending vibrations of CH_2 groups. Two lines of equal intensity at 1092 and 1035 cm^{-1} are attributed to the C–O bond vibrations in the $[OCH_2CH_2O]^{2-}$ ion in the Raman spectra of $Ti_{1-x}Mn_x(OCH_2CH_2O)_{2-x}$ with $x = 0.016$ and $Ti(OCH_2CH_2O)_2$. The intense lines at 925 and 885 cm^{-1} are due to the torsional vibrations of C–C bonds. No lines typical of the stretching and bending vibrations of OH groups in ethylene glycol were detected in the spectra.[14,15]

The thermolysis of $Ti_{1-x}Mn_x(OCH_2CH_2O)_{2-x}$ ($0.003 \leqslant x \leqslant 0.016$) in air at 500 °C was completed by the formation of $Ti_{1-x}Mn_xO_{2-x}$ solid solutions having an anatase structure according to the X-ray phase and Raman spectroscopic data (Figure 1). The Raman spectra of $Ti_{1-x}Mn_xO_{2-x}$ samples exhibited lines corresponding to the anatase structure [147 (E_g), 399 (B_{1g}), 516 (A_{1g}), and 639 cm^{-1} (E_g)]. As the dopant concentration was increased, the shape of the Raman spectrum changed. The Raman modes broadened, while the line intensity decreased to indicate the inclusion of manganese into the crystal lattice of titanium dioxide as a result of structure deformation. When the heat treatment temperature was raised to 700 °C, the Raman spectra contained lines typical of rutile [446 (E_g) and 611 cm^{-1} (A_{1g})] along with anatase modes. As the concentration of manganese was increased, the rutile content of the samples decreased; that is, manganese doping stabilizes the anatase phase of titanium dioxide.

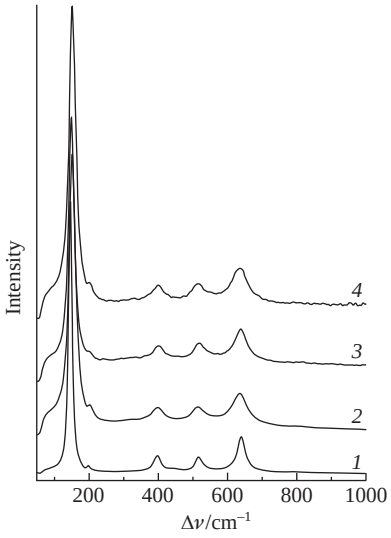

Figure 1 Raman spectra of the $Ti_{1-x}Mn_xO_{2-x}$ solid solutions: (*1*) $x = 0$, (*2*) $x = 0.003$, (*3*) $x = 0.0065$, and (*4*) $x = 0.016$.

An analysis of the SEM images of $Ti_{1-x}Mn_xO_{2-x}$ showed that the enhancement of manganese concentration has a considerable influence on the morphological and dimensional characteristics of solid solution particles. At small manganese concentrations ($x \leqslant 0.0035$), the particle shape was nearly spherical, but the spherical particles gradually delaminated into extended plates forming loose agglomerates as the dopant concentration was increased.

In order to determine the effect of manganese concentration on the absorption of titanium dioxide, we examined the absorption spectra of $Ti_{1-x}Mn_xO_{2-x}$ solid solution samples in the UV and visible spectral regions. The optical absorption spectra of $Ti_{1-x}Mn_xO_{2-x}$ ($x = 0$–0.016) samples synthesized by the annealing of $Ti_{1-x}Mn_x(OCH_2CH_2O)_{2-x}$ at 500 °C in air [Figure 2(*a*)] consisted of two broad absorption bands in the visible range, which correspond to the *d*–*d* transitions of the Mn^{2+} ion in the anatase matrix. The absorption observed at 370–470 nm was due to the $^6A_{1g}(S) \rightarrow {}^4A_{1g}(G)$, $^4E_g(G)$ and $^6A_{1g}(S) \rightarrow {}^4T_{2g}(G)$ transitions, whereas a maximum at 470–700 nm was due to the $^6A_{1g}(S) \rightarrow {}^4T_{1g}(G)$ transition in the Mn^{2+} ion. The growth of the concentration of manganese led to the displacement of the absorption band edge of anatase into the long-wavelength region, which points to the band gap.

To estimate the effective band gap of $Ti_{1-x}Mn_xO_{2-x}$, the experimental absorption spectra were brought to the form $(\alpha h\nu)^2 = f(h\nu)$. The dependence of the absorption coefficient of titanium dioxide as a direct band semiconductor on frequency near the absorption edge is described by the equation $\alpha(\nu) = [A(h\nu - E_g)^{1/2}]/h\nu$, where α is the absorption coefficient, $h\nu$ is the photon energy, E_g is the band gap, and A is the frequency ν independent constant. By extrapolating the linear portions of the curve to intersection with the abscissa axis in the long-wave part of the spectrum, we determined the band gap [Figure 2(*b*)]. When the concentration of manganese increased, the band gap of

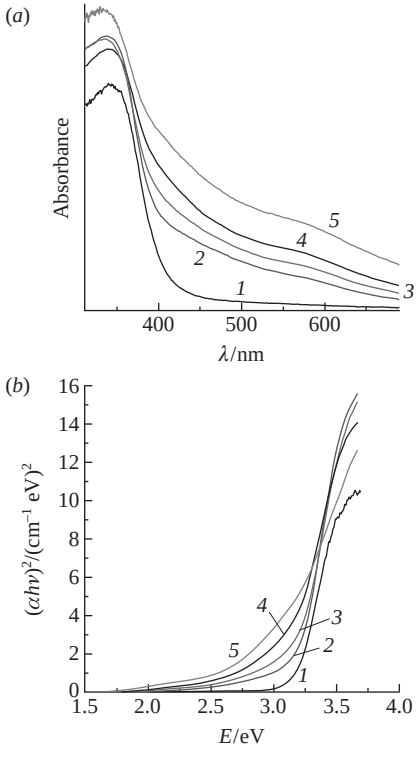

Figure 2 (*a*) Absorption spectra of the $Ti_{1-x}Mn_xO_{2-x}$ solid solutions in the UV and visible spectral regions; (*b*) $(\alpha h\nu)^2 = f(h\nu)$. (*1*) $x = 0$, (*2*) $x = 0.0035$, (*3*) $x = 0.0065$, (*4*) $x = 0.011$, and (*5*) $x = 0.016$.

† The phase analysis of the synthesized samples was carried out with the use of a POLAM S-112 polarization microscope in transmitted light and a STADI-P automatic X-ray diffractometer (STOE, Germany) in $CuK\alpha_1$ radiation. The particle size and shape of the precursors and their thermolysis products were determined by scanning electron microscopy on a JSM5900LV instrument. The diffuse reflection spectra were recorded in a range of 190–800 nm on a UV-3600 spectrometer (Shimadzu; $\lambda = 310$ nm) using $BaSO_4$ as a standard substance. The Raman spectra were obtained at room temperature on a RAMII module attachment compatible with a Vertex 80 Fourier transform IR spectrometer ($\lambda = 1064$ nm, Nd:YAG, $P = 450$ mW). The photocatalytic activity of $Ti_{1-x}Mn_xO_{2-x}$ was estimated from the oxidation reaction of water-dissolved hydroquinone during irradiation in both UV and visible regions using a BUF-15 mercury lamp ($\lambda_{max} = 253$ nm) and a blue luminescence lamp ($\lambda_{max} = 425$ nm), respectively.[10–12]

$Ti_{1-x}Mn_xO_{2-x}$ regularly lowered: 3.22, 3.09, 2.97, 2.89 and 2.72 eV at x = 0, 0.0035, 0.0065, 0.011 and 0.016, respectively. Consequently, doping with manganese effectively expands the optical absorption of anatase into the visible spectral region.

The examination of the photocatalytic activity of the synthesized $Ti_{1-x}Mn_xO_{2-x}$ solid solution samples with the anatase structure in the oxidation reaction of water-dissolved hydroquinone in the UV and visible spectral regions revealed that the introduction of manganese into the titanium dioxide structure and an increase in its concentration enhanced the photocatalyst activity (Figure 3). Manganese has several valence states that can trap electrons or holes; as a result, the photoactivity grows. Moreover, the activity of Mn^{2+} can be due to the half-filled valence electron configuration $3d^5 4s^2$, which leads to the formation of highly reactive particles. The electron configuration changes to d^6 when manganese acts as an electron trapping site, and to d^4, if it is a hole trap. For the restoration of a stable electron configuration, an electron is trapped by oxygen molecules giving rise to superoxide radicals (O_2^-), whereas a hole is absorbed by water molecules adsorbed on the surface to generate ·OH radicals:

$$Mn^{2+} + e^- \rightarrow Mn^+,$$

$$Mn^+ + O_2 \rightarrow Mn^{2+} + O_2^-,$$

$$Mn^{2+} + h^+ \rightarrow Mn^{3+},$$

$$Mn^{3+} + OH^- \rightarrow Mn^{2+} + {}^{\cdot}OH.$$

The activity of a commercial Degussa P25 photocatalyst under UV irradiation is much lower [Figure 3(*a*)], and it is almost inactive in the visible spectral region [Figure 3(*b*)]. The hydroquinone oxidation rate under UV irradiation is consideravly higher than that in visible light, and the oxide with a maximal concentration of manganese (x = 0.016) exhibits the highest photocatalytic activity. Under irradiation with visible light, the photocatalytic activity increased more slowly with the dopant concentration, and it terminated at $x \geqslant 0.011$ in spite of the red shift of the optical absorption edge. Therefore, the optical absorption and the photocatalytic activity of $Ti_{1-x}Mn_xO_{2-x}$ largely depend on the concentration of manganese, and the defects formed at a high concentration of Mn serve as recombination centers to suppress the photoactivity. The defect levels in TiO_2 become localized, and the trapped carriers cannot migrate to the surface to participate in photocatalysis.

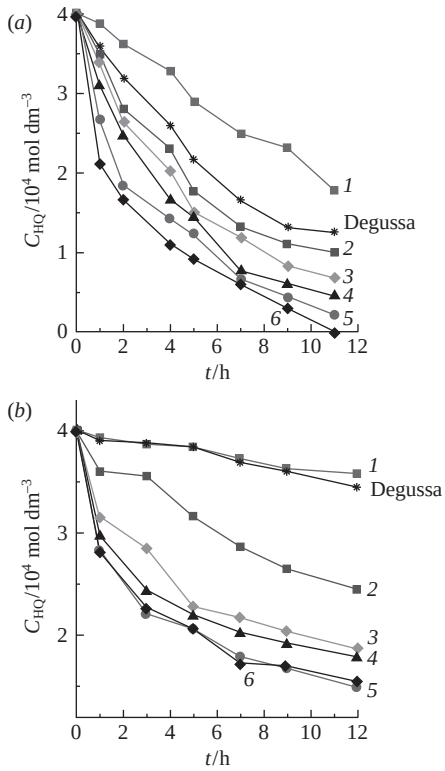

Figure 3 The time dependence of hydroquinone concentration under the (*a*) UV and (*b*) visible light irradiation of solutions (*1*) without catalyst and in the presence of the $Ti_{1-x}Mn_xO_{2-x}$ powders: (*2*) x = 0, (*3*) x = 0.0035, (*4*) x = 0.0065, (*5*) x = 0.011, and (*6*) x = 0.016.

Thus, the photocatalytic activity of $Ti_{1-x}Mn_xO_{2-x}$ solid solution (x = 0.003–0.016) samples with the anatase structure synthesized by a precursor method considerably exceeds that of the commercial Degussa P25 photocatalyst under UV irradiation and is rather high in the visible spectral region, in which the Degussa P25 catalyst is not active at all. The shape of the precursor crystals depends not only on the synthesis conditions but also on the concentration of manganese. Nevertheless, the thermolysis of a $Ti_{1-x}Mn_x(OCH_2CH_2O)_{2-x}$ precursor in air is a pseudomorphic process; that is, the resulting oxide particles inherited the shape of its crystal aggregates.

References

1 Y. Ma, X. Wang, Y. Jia, X. Chen, H. Han and C. Li, *Chem. Rev.*, 2014, **114**, 9987.
2 H. Huang, H. Huang, L. Zhang, P. Hu, X. Ye and D. Y. C. Leung, *Chem. Eng. J*., 2015, **259**, 534.
3 V. D. Binas, K. Sambani, T. Maggos, A. Katsanaki and G. Kiriakidis, *Appl. Catal. B*, 2012, **113**–**114**, 79.
4 H. Feng, M. H. Zhang and L. E. Yu, *Appl. Catal. A*, 2012, **413**–**414**, 238.
5 K. Nagaveni, M. S. Hegde and G. Madras, *J. Phys. Chem. B*, 2004, **108**, 20204.
6 O. I. Gyrdasova, V. N. Krasil'nikov, E. V. Shalaeva, I. V. Baklanova, M. A. Melkozerova, L. Yu. Buldakova and M. Yu. Yanchenko, *Mendeleev Commun*., 2014, **24**, 143.
7 N. Luo, H. W. Jing, Z. G. Ma, W. Liu, L. Zhang and G. Sun, *Mendeleev Commun*., 2016, **26**, 157.
8 I. V. Baklanova, V. N. Krasil'nikov, V. P. Zhukov, O. I. Gyrdasova, L. A. Perelyaeva, L.Yu. Buldakova, M. Yu. Yanchenko and I. R. Shein, *Russ. J. Inorg. Chem.*, 2014, **59**, 29 (*Zh. Neorg. Khim*., 2014, **59**, 154).
9 V. N. Krasil'nikov, V. P. Zhukov, I. V. Baklanova, O. I. Gyrdasova and L. Yu. Buldakova, *Catal. Lett*., 2015, **145**, 1290.
10 V. N. Krasil'nikov, A. P. Shtin, O. I. Gyrdasova, E. V. Polyakov and G. P. Shveikin, *Russ. J. Inorg. Chem*., 2008, **53**, 1065 (*Zh. Neorg. Khim.*, 2008, **53**, 1146).
11 V. N. Krasil'nikov, O. I. Gyrdasova, I. V. Baklanova, L.Yu. Buldakova, M. Yu. Yanchenko, R. F. Samigullina and O. V. Koryakova, *Russ. J. Inorg. Chem*., 2013, **58**, 120 (*Zh. Neorg. Khim*., 2013, **58**, 154).
12 I. V. Baklanova, V. N. Krasil'nikov, V. P. Zhukov, O. I. Gyrdasova, M. V. Kuznetsov, L. Yu. Buldakova and M. Yu. Yanchenko, *J. Photochem. Photobiol. A*, 2016, **314**, 6.
13 D. Wang, Yu. Ranbo, N. Kumada and N. Kinomura, *Chem. Mater*., 1999, **11**, 2008.
14 K. Krishnan and R. S. Krishnan, *Proc. Indian Acad. Sci.*, 1966, **64**, 111.
15 H. Matsuura and T. Miyazawa, *Bull. Chem. Soc. Jpn*., 1967, **40**, 85.

Received: 19th January 2016; Com. 16/4819